IEEE Access
Multidisciplinary ⋮ Rapid Review ⋮ Open Access Journal

Received April 10, 2022, accepted April 17, 2022, date of publication April 21, 2022, date of current version April 28, 2022.

Digital Object Identifier 10.1109/ACCESS.2022.3169150

Continuous Sliding Mode Control of Robotic Manipulators Based on Time-Varying Disturbance Estimation and Compensation

JUAN XIAN[1,2], LI SHEN[2], JUNLIN CHEN[2], AND WENGUO FENG[2]
[1]Chongqing Key Laboratory of Public Big Data Security Technology, Chongqing College of Mobile Telecommunication, Chongqing 401520, China
[2]College of Communication and Information Engineering, Chongqing College of Mobile Telecommunication, Chongqing 401520, China

Corresponding author: Juan Xian (jianxuanbb@163.com)

This work was supported in part by the Research Project of Higher Education Teaching Reform of Chongqing University of Mobile Education, China, under Grant YTJG201813 and Grant YTJG201914; in part by the Science and Technology Research Project of Chongqing Education Commission under Grant KJZD-M202001901; and in part by the General Projects of Chongqing Science and Technology Commission under Grant cstc2020jcyj-msxmX0895.

ABSTRACT To address the high-precision trajectory tracking task of uncertain robotic manipulators, a continuous sliding mode control (CSMC) scheme based on time-varying disturbance estimation and compensation is developed. The proposed control approach can not only avoid the chattering of the traditional sliding mode control (SMC) scheme and solve the problems existing in the application of the CSMC method but also make the robot obtain stronger disturbance rejection performance. Meanwhile, the stability of the closed-loop system under the recommended control approach is guaranteed by a defined Lyapunov function. Finally, the trajectory tracking and disturbance rejection performance of the 2-DOF robot under the action of the PID control, traditional SMC, CSMC, and present control methods are carried out, respectively. The results show the effectiveness and superiority of the proposed control method.

INDEX TERMS Continuous sliding mode control (CSMC), time-varying disturbances, disturbance estimation, trajectory tracking.

I. INTRODUCTION

With the development of science and technology, robots have been widely used in traditional industrial fields such as handling, palletizing, welding, and so on. Meanwhile, they have gradually infiltrated into application fields such as human-machine interaction and collaboration [1]–[4]. Correspondingly, higher requirements have been put forward for the control performance of robots [5]–[7]. However, the robot system is a multi-variable and state-coupled nonlinear system, which means it is difficult to obtain an accurate dynamic model [8], [9]. Therefore, the use of linear control methods such as proportional-integral-derivative (PID) control cannot make the system achieve satisfactory control performance [10], [11]. At the same time, there are inevitably various parameter uncertainties and external disturbances in the robot system, this factor further increases the difficulty of the controller design [12].

Aiming at the trajectory tracking problem of robots, many nonlinear control schemes, such as backstepping control, adaptive control, sliding mode control (SMC), and neural network control, have been proposed by scholars [13]–[16]. However, these nonlinear control methods generally passively suppress disturbances through feedback and cannot actively deal with system disturbances [17]. Among these nonlinear control methods, SMC scheme has attracted more and more attention due to its simple design, easy parameter adjustment, and ability to actively deal with system internal parameter uncertainties and external disturbances [18]–[20]. However, to a certain extent, its extensive promotion in the actual system is limited because of the chattering phenomenon of the traditional SMC method [21], [22]. In order to solve this problem, researchers have proposed many SMC methods based on chattering suppression or attenuation, such as the saturation function-based SMC method, adaptive control gain-based SMC strategy, and continuous SMC (CSMC) scheme based on continuous control behavior [23]–[25]. Although these improved methods can reduce the chattering of a system, there are still some shortcomings. For example, the saturation function-based SMC method reduces the system robustness to a certain extent, the sliding mode control method based on the adaptive gain is still a

The associate editor coordinating the review of this manuscript and approving it for publication was Shihong Ding.

discontinuous control rate in nature, and the CSMC approach has problems of implementation cost and computational burden.

Considering that various disturbances in the robot system will adversely affect its control performance [26], [27], many effective disturbance estimation methods have been proposed, such as disturbance observer (DO) that estimates disturbances based on the nominal model of the system, extended state observer (ESO) that can estimate the system state and disturbance, generalized proportional integral observer (GPIO) for observing the time-varying disturbance and system states, and high-order sliding mode observer (HOSMO) for the estimation of time-varying disturbance in a finite time [28]–[30]. These disturbance estimation methods have their different characteristics. In actual application, the appropriate observer can be selected according to the characteristics of the studied systems [31]–[35].

In this work, a high-precision trajectory tracking control strategy based on the GPIO and CSMC technique is proposed for a disturbed robotic manipulator. First, considering the various time-varying disturbances in the robot, a GPIO derived from the expanded robot dynamics model is developed to estimate unknown time-varying disturbances and unmeasured states of the system. Then, a new dynamic sliding mode surface and a new continuous sliding mode controller based on the estimated values are designed, respectively. The stability proof of the closed-loop system under the recommended control method is also given. Finally, four control schemes including PID control, traditional SMC, CSMC, and recommended control algorithms are tested and compared respectively on a two-link rigid robot. The results show that the designed control algorithm possesses fast tracking performance and strong disturbance rejection capability.

The rest of this article is organized as follows. In Section II, a dynamic model description of a class of n-link rigid robotic manipulators is firstly presented. Section III introduces the existing problem of the traditional SMC and CSMC methods respectively. The design process of the proposed control scheme including the design of a multi-functional observer, a recommended CSMC law, and stability analysis is provided in Section IV. Test results between the present control approach and other methods are shown in Section V. Finally, VI concludes the work.

II. DYNAMIC MODEL DESCRIPTION

Consider a class of n-link rigid robotic manipulators based on Euler-Lagrange equations, the dynamic model is obtained as [12]:

$$\boldsymbol{M}(\boldsymbol{q})\ddot{\boldsymbol{q}} + \boldsymbol{C}(\boldsymbol{q}, \dot{\boldsymbol{q}})\dot{\boldsymbol{q}} + \boldsymbol{G}(\boldsymbol{q}) = \boldsymbol{u}(t) + \boldsymbol{d}(t), \tag{1}$$

where $\boldsymbol{q}$, $\dot{\boldsymbol{q}}$, $\ddot{\boldsymbol{q}} \in R^n$ represent the robot joint angle, angular velocity and angular acceleration, respectively; $\boldsymbol{M}(\boldsymbol{q}) \in R^{n\times n}$ represents inertia matrix; $\boldsymbol{C}(\boldsymbol{q}, \dot{\boldsymbol{q}}) \in R^{n\times n}$ represents Coriolis force and centrifugal force matrix; $\boldsymbol{G}(\boldsymbol{q}) \in R^n$ stands for gravity vector; $\boldsymbol{u}(t) \in R^n$ denotes joint control torque; $\boldsymbol{d}(t) \in R^n$ stands for unknown disturbances, including robot external disturbances and unmodeled dynamics [36].

Due to the uncertain parameters of the actual robot, the parameters $\boldsymbol{M}(\boldsymbol{q})$, $\boldsymbol{C}(\boldsymbol{q}, \dot{\boldsymbol{q}})$, and $\boldsymbol{G}(\boldsymbol{q})$ can be defined as:

$$\begin{cases} \boldsymbol{M}(\boldsymbol{q}) = \boldsymbol{M}_0(\boldsymbol{q}) + \Delta\boldsymbol{M}(\boldsymbol{q}), \\ \boldsymbol{C}(\boldsymbol{q}, \dot{\boldsymbol{q}}) = \boldsymbol{C}_0(\boldsymbol{q}, \dot{\boldsymbol{q}}) + \Delta\boldsymbol{C}(\boldsymbol{q}, \dot{\boldsymbol{q}}), \\ \boldsymbol{G}(\boldsymbol{q}) = \boldsymbol{G}_0(\boldsymbol{q}) + \Delta\boldsymbol{G}(\boldsymbol{q}), \end{cases} \tag{2}$$

where $\boldsymbol{M}_0(\boldsymbol{q})$, $\boldsymbol{C}_0(\boldsymbol{q}, \dot{\boldsymbol{q}})$, and $\boldsymbol{G}_0(\boldsymbol{q})$ represent the nominal value of parameters; $\Delta\boldsymbol{M}(\boldsymbol{q})$, $\Delta\boldsymbol{C}(\boldsymbol{q}, \dot{\boldsymbol{q}})$ and $\Delta\boldsymbol{G}(\boldsymbol{q})$ represent the uncertainty of parameters. Based on formula (2), dynamics equation (1) can be rearranged as:

$$\boldsymbol{M}_0(\boldsymbol{q})\ddot{\boldsymbol{q}} + \boldsymbol{C}_0(\boldsymbol{q}, \dot{\boldsymbol{q}})\dot{\boldsymbol{q}} + \boldsymbol{G}_0(\boldsymbol{q}) = \boldsymbol{u}(t) + \boldsymbol{w}(t), \tag{3}$$

where $\boldsymbol{w}(t) = \boldsymbol{d}(t) - \Delta\boldsymbol{M}(\boldsymbol{q})\ddot{\boldsymbol{q}} - \Delta\boldsymbol{C}(\boldsymbol{q}, \dot{\boldsymbol{q}})\dot{\boldsymbol{q}} - \Delta\boldsymbol{G}(\boldsymbol{q})$, which includes uncertain internal parameters of the system, external disturbances and unmodeled dynamics.

Define the tracking error of the system as $\boldsymbol{e}_1 = \boldsymbol{q}_r - \boldsymbol{q}$, where $\boldsymbol{q}_r = [q_{r1}, q_{r2}, \ldots q_{rn}]^T$ is the reference trajectory. Assuming that $\boldsymbol{q}_r$ is second-order differentiable, the dynamic model (3) can be described as follows:

$$\begin{cases} \dot{\boldsymbol{e}}_1 = \boldsymbol{e}_2, \\ \dot{\boldsymbol{e}}_2 = \ddot{\boldsymbol{q}}_r - \boldsymbol{M}_0^{-1}(\boldsymbol{e}_1)\boldsymbol{u}(t) + \boldsymbol{F}(\boldsymbol{e}_1, \boldsymbol{e}_2) + \boldsymbol{D}(t), \end{cases} \tag{4}$$

where $\boldsymbol{e} = [\boldsymbol{e}_1^T, \boldsymbol{e}_2^T]^T$, $\boldsymbol{F}(\boldsymbol{e_1}, \boldsymbol{e_2}) = \boldsymbol{M}_0^{-1}(\boldsymbol{e}_1)[\boldsymbol{C}_0(\boldsymbol{e}_1, \boldsymbol{e}_2)e_2 + \boldsymbol{G}_0(\boldsymbol{e})]$, $\boldsymbol{D}(t) = -\boldsymbol{M}_0^{-1}(\boldsymbol{q})\boldsymbol{w}(t) = -\boldsymbol{M}_0^{-1}(\boldsymbol{q})[\boldsymbol{d}(t) - \Delta\boldsymbol{M}(\boldsymbol{q})\ddot{\boldsymbol{q}} - \Delta\boldsymbol{C}(\boldsymbol{q}, \dot{\boldsymbol{q}})\dot{\boldsymbol{q}} - \Delta\boldsymbol{G}(\boldsymbol{q})]$ is the lumped disturbances including internal and external disturbances in the system.

The research goal of this paper is to design a high-precision trajectory tracking controller based on the estimation and compensation of time-varying disturbances to make the tracking error $\boldsymbol{e}_1 = \boldsymbol{q}_r - \boldsymbol{q}$ in system (4) asymptotically approach zero, that is, position output $\boldsymbol{q}$ of the robot system can track its reference trajectory $\boldsymbol{q}_r$, effectively. Next on, we will first analyze the problems existing in the SMC and CSMC methods when it is applied to dynamic equation (4), and then the recommended control law will be proposed in this article.

III. EXISTING PROBLEMS IN SMC METHODS

A. EXISTING PROBLEMS IN TRADITIONAL SMC METHODS

Assumption 1 [37]: For the lumped disturbance $\boldsymbol{D}(t)$ in system (4), there is a positive number κ_{d_1}, which satisfies $||\boldsymbol{D}(t)|| \leq \kappa_{d_1}$. The design of the SMC method generally includes two steps: the design of the sliding mode surface and the design of the SMC law.

First, we design the sliding mode surface as:

$$\begin{cases} \boldsymbol{\sigma} = \boldsymbol{e}_2 + \boldsymbol{\lambda}\boldsymbol{e}_1, \\ \boldsymbol{e}_2 = \dot{\boldsymbol{q}}_r - \dot{\boldsymbol{q}}, \boldsymbol{e}_1 = \boldsymbol{q}_r - \boldsymbol{q}, \end{cases} \tag{5}$$

where $\boldsymbol{\lambda} = diag(\lambda_1, \lambda_2 \ldots, \lambda_n)$, $\lambda_i > 0$ is the parameter that needs to be configured. Then the traditional SMC law is given as [38]:

$$\boldsymbol{u}(t) = \boldsymbol{M}_0(\boldsymbol{e}_1)(\ddot{\boldsymbol{q}}_r + \boldsymbol{F}(\boldsymbol{e}_1, \boldsymbol{e}_2) + \boldsymbol{\lambda}\boldsymbol{e}_2 + \kappa sign(\boldsymbol{\sigma})), \tag{6}$$

where $\boldsymbol{\kappa} = diag(\kappa_1, \kappa_2, \ldots \kappa_n)$, $\kappa_i > 0$ is the controller parameter, $sign(*)$ is a standard symbolic function.

Let $\underline{\kappa}_1 = min(\kappa_i)$, according to **Assumption 1**, if $\underline{\kappa}_1 > \kappa_{d_1}$, the tracking error $\boldsymbol{e}_1$ of the robot system will converge to the designed sliding surface $\boldsymbol{\sigma} = \boldsymbol{e}_2 + \boldsymbol{\lambda}\boldsymbol{e}_1 = \boldsymbol{0}$ in a finite time. Meanwhile, because of $\lambda_i > 0$, the tracking error $\boldsymbol{e}_1$ will asymptotically approach zero along with the sliding surface after reaching the sliding surface $\boldsymbol{\sigma} = \boldsymbol{0}$, which means system output $\boldsymbol{q}$ will asymptotically converge to $\boldsymbol{q}_r$.

Remark 1: From the designed sliding mode controller (6), it is well known that the traditional SMC method has a discontinuous control behavior due to the high-frequency switching function (symbolic function), which may cause chattering or even more serious problems such as the actuator in the system is permanently damaged or the system cannot operate normally. Therefore, it is extremely important to design an SMC method with continuous control behavior for the robot control system.

B. EXISTING PROBLEMS IN CSMC METHODS

Assumption 2 [39]: For the lumped disturbance $\boldsymbol{D}(t)$ in system (4), there is a positive number κ_{d_2} that satisfies condition $||\dot{\boldsymbol{D}}(t)|| \leq \kappa_{d_2}$.

First, the sliding mode surface is designed as:

$$\begin{cases} \boldsymbol{\sigma} = \dot{\boldsymbol{e}}_2 + \boldsymbol{\lambda}_2\boldsymbol{e}_2 + \boldsymbol{\lambda}_1\boldsymbol{e}_1, \\ \boldsymbol{e}_2 = \dot{\boldsymbol{q}}_r - \dot{\boldsymbol{q}}, \boldsymbol{e}_1 = \boldsymbol{q}_r - \boldsymbol{q}, \end{cases} \tag{7}$$

where $\boldsymbol{\lambda}_1 = diag(\lambda_{11}, \lambda_{12}, \ldots, \lambda_{1n})$, $\boldsymbol{\lambda}_2 = diag(\lambda_{21}, \lambda_{22}, \ldots, \lambda_{2n})$, The configuration principle of $\lambda_{1i}, \lambda_{2i} > 0$. $\lambda_{ij}(i = 1, 2, j = 1, 2, \ldots, n)$ is to make all the characteristic roots of the characteristic polynomial $p(s) = s^2 + \lambda_{2i}s + \lambda_{1i}$ lie on the left half of the complex plane s. Then, the CSMC law is designed as [23]:

$$\begin{cases} \boldsymbol{u}(t) = \boldsymbol{u}_{eq}(t) + \boldsymbol{u}_v(t), \\ \boldsymbol{u}_{eq}(t) = \boldsymbol{M}_0(\boldsymbol{e}_1)(\ddot{\boldsymbol{q}}_r + \boldsymbol{F}(\boldsymbol{e}_1, \boldsymbol{e}_2) + \boldsymbol{\lambda}_2\boldsymbol{e}_2 + \boldsymbol{\lambda}_1\boldsymbol{e}_1), \\ \dot{\boldsymbol{u}}_v(t) = \boldsymbol{M}_0(\boldsymbol{e}_1)\boldsymbol{\kappa} sign(\boldsymbol{\sigma}), \end{cases} \tag{8}$$

where $\boldsymbol{\kappa} = diag(\kappa_1, \kappa_2 \ldots \kappa_n)$, $\kappa_i > 0$ is the controller parameter.

Let $\underline{\kappa}_2 = min(\kappa_i)$, according to **Assumption 2**, if $\underline{\kappa}_2 > \kappa_{d_2}$, the tracking error $\boldsymbol{e}_1$ of the robot system will converge to the designed sliding surface $\boldsymbol{\sigma} = \dot{\boldsymbol{e}}_2 + \boldsymbol{\lambda}_2\boldsymbol{e}_2 + \boldsymbol{\lambda}_1\boldsymbol{e}_1 = 0$ in a finite time. Due to $\lambda_{1i}, \lambda_{2i} > 0$, the tracking error $\boldsymbol{e}_1$ will continue to approach zero along with the sliding surface $\boldsymbol{\sigma} = 0$ under the control law (8), which means system output $\boldsymbol{q}$ will converge to $\boldsymbol{q}_r$ in an asymptotic manner.

Remark 2: Compared with the traditional SMC method shown in formula (6), the CSMC method of formulas (7) and (8) can eliminate the chattering phenomenon because it can provide continuous control behavior. However, there are two limitations when the CSMC method is applied to the actual systems: 1) In order to effectively suppress system disturbances, the controller (8) is generally configured with a larger control gain $\boldsymbol{\kappa}$, which will result in a larger steady-state tracking error; 2) Noted that formulas (7) and (8) include the first and second derivatives, $\dot{\boldsymbol{q}}$, $\ddot{\boldsymbol{q}}$ of system output $\boldsymbol{q}$, but in actual systems, speed, and acceleration sensors are generally not installed due to the factors such as cost and maintenance. Although the literature [23] gives a solution to solve this problem, it still increases the computational burden of the system.

IV. DESIGN OF CSMC BASED ON DISTURBANCE ESTIMATION AND COMPENSATION

In order to cope with the shortcomings of the traditional SMC and CSMC methods in practical applications, a composite control method based on the combination of the GPIO and CSMC is proposed. The design steps of the recommended control strategy and corresponding theoretical analysis are given below.

A. ESTIMATION OF TIME-VARYING DISTURBANCE AND STATES

Assumption 3 [1]: For the lumped disturbance $\boldsymbol{D}(t)$ in system (4), it is assumed that its m order is differentiable.

Consider that the robot system is often affected by time-varying disturbances, and in order to reduce the computational burden, a GPIO is designed to estimate the unmeasured state of the system and time-varying disturbances. According to **Assumption 3**, define a new set of state variables: $\boldsymbol{\eta}_1 = \boldsymbol{e}_1$, $\boldsymbol{\eta}_2 = \boldsymbol{e}_2$, $\boldsymbol{\eta}_3 = \boldsymbol{D}(t)$, $\boldsymbol{\eta}_4 = \dot{\boldsymbol{D}}(t)$, $\cdots$, $\boldsymbol{\eta}_{m+1} = \boldsymbol{D}^{(m-2)}(t)$, $\boldsymbol{\eta}_{m+2} = \boldsymbol{D}^{(m-1)}(t)$, Then system (4) can be expanded to:

$$\begin{cases} \dot{\boldsymbol{\eta}}_1 = \boldsymbol{\eta}_2, \\ \dot{\boldsymbol{\eta}}_2 = \boldsymbol{\eta}_3 + \ddot{\boldsymbol{q}}_r - \boldsymbol{M}_0^{-1}(\boldsymbol{\eta}_1)\boldsymbol{u}(t) + \boldsymbol{F}(\boldsymbol{\eta}_1, \boldsymbol{\eta}_2), \\ \dot{\boldsymbol{\eta}}_3 = \boldsymbol{\eta}_4, \dot{\boldsymbol{\eta}}_4 = \dot{\boldsymbol{\eta}}_5, \cdots, \\ \dot{\boldsymbol{\eta}}_{m+1} = \boldsymbol{\eta}_{m+2}, \\ \dot{\boldsymbol{\eta}}_{m+2} = \boldsymbol{D}^{(m)}(t), \end{cases} \tag{9}$$

Based on the expanded state-space equation (9), a GPIO can be designed as [40]:

$$\begin{cases} \dot{\hat{\boldsymbol{\eta}}}_1 = \hat{\boldsymbol{\eta}}_2 + \boldsymbol{c}_{m+2}(\boldsymbol{\eta}_1 - \hat{\boldsymbol{\eta}}_1), \\ \dot{\hat{\boldsymbol{\eta}}}_2 = \hat{\boldsymbol{\eta}}_3 + \ddot{\boldsymbol{q}}_r - \boldsymbol{M}_0^{-1}(\boldsymbol{\eta}_1)\boldsymbol{u}(t) \\ \qquad + \boldsymbol{F}(\boldsymbol{\eta}_1, \hat{\boldsymbol{\eta}}_2) + \boldsymbol{c}_{m+1}(\boldsymbol{\eta}_1 - \hat{\boldsymbol{\eta}}_1), \\ \dot{\hat{\boldsymbol{\eta}}}_3 = \hat{\boldsymbol{\eta}}_4 + \boldsymbol{c}_m(\boldsymbol{\eta}_1 - \hat{\boldsymbol{\eta}}_1), \dot{\hat{\boldsymbol{\eta}}}_4 = \hat{\boldsymbol{\eta}}_5 + \boldsymbol{c}_{m-1}(\boldsymbol{\eta}_1 - \hat{\boldsymbol{\eta}}_1), \ldots, \\ \dot{\hat{\boldsymbol{\eta}}}_{m+1} = \hat{\boldsymbol{\eta}}_{m+2} + \boldsymbol{c}_2(\boldsymbol{\eta}_1 - \hat{\boldsymbol{\eta}}_1), \\ \dot{\hat{\boldsymbol{\eta}}}_{m+2} = \hat{\boldsymbol{\eta}}_{m+2} + \boldsymbol{c}_1(\boldsymbol{\eta}_1 - \hat{\boldsymbol{\eta}}_1), \end{cases} \tag{10}$$

where $\hat{\boldsymbol{\eta}}_1, \hat{\boldsymbol{\eta}}_2, \cdots, \hat{\boldsymbol{\eta}}_{m+1}, \hat{\boldsymbol{\eta}}_{m+2}$ represent the estimations of $\boldsymbol{\eta}_1$, $\boldsymbol{\eta}_2, \cdots, \boldsymbol{\eta}_{m+1}, \boldsymbol{\eta}_{m+2}$ respectively; the configuration principle of $\boldsymbol{c}_i(i = 1, 2, \cdots, m+2, j = 1, 2, \ldots, n)$ is that all the characteristic roots of the characteristic polynomial $p_0(s) = s^{m+2} + c_{(m+2)i}s^{m+1} + c_{(m+1)i}s^m + \cdots + c_{2i}s + c_{1i}$ lie on the left half of the complex plane s.

B. DESIGN OF RECOMMENDED CONTROLLER

With the aid of the estimations of system states and time-varying disturbances from GPIO (10), a new sliding surface

TABLE 1. The parameters of the controllers.

Parameters	Values
PID	$\boldsymbol{k}_D = diag(3p, 3p), \boldsymbol{k}_P = (3p^2, 3p^2)$ $\boldsymbol{k}_I = diag(p^3, p^3), p = 5$
SMC	$\boldsymbol{\lambda} = diag(5, 5), \boldsymbol{k} = diag(4, 4),$
CSMC	$\boldsymbol{\lambda}_2 = diag(2p, 2p), \boldsymbol{\lambda}_1 = diag(p^2, p^2),$ $p = 10, \boldsymbol{k} = diag(4, 4)$
CSMC+GPIO	$\boldsymbol{\lambda}_2 = diag(2p, 2p), \boldsymbol{\lambda}_1 = diag(p^2, p^2), p = 10,$ $\boldsymbol{c}_5 = diag(6\rho, 6\rho), \boldsymbol{c}_4 = diag(10\rho^2, 10\rho^2),$ $\boldsymbol{c}_3 = diag(10\rho^3, 10\rho^3), \boldsymbol{c}_2 = diag(5\rho^4, 5\rho^4),$ $\boldsymbol{c}_1 = diag(\rho^5, \rho^5), \rho = 2000, \boldsymbol{k} = diag(2, 2)$

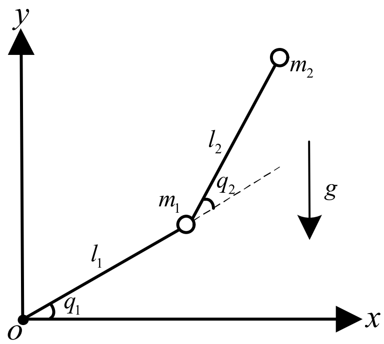

FIGURE 1. Two-link rigid robot.

can be constructed as shown below:

$$\begin{cases} \boldsymbol{\sigma} = \ddot{\boldsymbol{q}}_r - \boldsymbol{M}_0^{-1}(\boldsymbol{\eta}_1)\boldsymbol{u}(t) + \boldsymbol{F}(\boldsymbol{\eta}_1, \hat{\boldsymbol{\eta}}_2) \\ \qquad + \hat{\boldsymbol{\eta}}_3 + \boldsymbol{\lambda}_2\hat{\boldsymbol{\eta}}_2 + \boldsymbol{\lambda}_1\boldsymbol{\eta}_1, \\ \boldsymbol{e}_1 = \boldsymbol{q}_r - \boldsymbol{q}, \end{cases} \tag{11}$$

where $\boldsymbol{\lambda}_1$, $\boldsymbol{\lambda}_2$ are configured in the same principle as the coefficients in formula (7). Then, a CSMC law based on disturbance estimation and compensation can be designed as:

$$\begin{cases} \boldsymbol{u}(t) = \boldsymbol{u}_{eq}(t) + \boldsymbol{u}_v(t), \\ \boldsymbol{u}_{eq}(t) = \boldsymbol{M}_0(\boldsymbol{\eta}_1)(\ddot{\boldsymbol{q}}_r + \boldsymbol{F}(\boldsymbol{\eta}_1, \hat{\boldsymbol{\eta}}_2)) + \hat{\boldsymbol{\eta}}_3 + \boldsymbol{\lambda}_2\hat{\boldsymbol{\eta}}_2 + \boldsymbol{\lambda}_1\boldsymbol{\eta}_1, \\ \dot{\boldsymbol{u}}_v(t) = \boldsymbol{M}_0(\boldsymbol{\eta}_1)\boldsymbol{\kappa} sign(\boldsymbol{\sigma}), \end{cases} \tag{12}$$

where $\boldsymbol{\kappa} = diag(\kappa_1, \kappa_2, \ldots, \kappa)$, κ_i is the controller parameter.

The stability analysis of the closed-loop system under the recommended control law is given below.

Lemma 1 [41]: Given an Input-to-State Stable (ISS) nonlinear system $\dot{x} = \zeta(x, v)$, if system input v satisfies the condition $\lim_{t\to\infty} v(t) = 0$, then we can get $\lim_{t\to\infty} x(t) = 0$.

Theorem 1: For a given robot system (3), GPIO (10), dynamic sliding surface (11) and composite controller (12) can be designed separately. When coefficients $\boldsymbol{c}_i$ in GPIO (10) and coefficients $\boldsymbol{\lambda}_i$ in sliding mode surface (11) are configured appropriately, if coefficients $\boldsymbol{\kappa}$ in controller (12) meet the condition $min(\kappa_i) > 0$, the system tracking error $\boldsymbol{e}_1$ will approach zero along with sliding surface under control law (12), which means system output $\boldsymbol{q}$ will asymptotically converge to $\boldsymbol{q}_r$.

Proof: First, substituting the designed control law (12) into the sliding surface (11), we can get:

$$\begin{aligned} \boldsymbol{\sigma} &= \ddot{\boldsymbol{q}}_r - \boldsymbol{M}_0^{-1}(\boldsymbol{\eta}_1)\boldsymbol{u}(t) + \boldsymbol{F}(\boldsymbol{\eta}_1, \hat{\boldsymbol{\eta}}_2) + \hat{\boldsymbol{\eta}}_3 + \boldsymbol{\lambda}_2\hat{\boldsymbol{\eta}}_2 + \boldsymbol{\lambda}_1\boldsymbol{\eta}_1, \\ &= \ddot{\boldsymbol{q}}_r - \boldsymbol{M}_0^{-1}(\boldsymbol{\eta}_1)(\boldsymbol{u}_{eq}(t) + \boldsymbol{u}_v(t)) + \boldsymbol{F}(\boldsymbol{\eta}_1, \hat{\boldsymbol{\eta}}_2) \\ &\quad + \hat{\boldsymbol{\eta}}_3 + \boldsymbol{\lambda}_2\hat{\boldsymbol{\eta}}_2 + \boldsymbol{\lambda}_1\boldsymbol{\eta}_1, \\ &= -\boldsymbol{M}_0^{-1}(\boldsymbol{\eta}_1)\boldsymbol{u}_v(t). \end{aligned} \tag{13}$$

Taking the derivative of the above formula and plugging in $\dot{u}_v(t)$ from formula (12), we can obtain:

$$\dot{\boldsymbol{\sigma}} = -\boldsymbol{\kappa} sign(\boldsymbol{\sigma}). \tag{14}$$

Next on, define a Lyapunov function $V = 0.5\boldsymbol{\sigma}^T\boldsymbol{\sigma}$, then take the derivative of V, yields:

$$\begin{aligned} \dot{V} &= \boldsymbol{\sigma}^T\dot{\boldsymbol{\sigma}} = \boldsymbol{\sigma}^T(-\boldsymbol{\kappa} sign(\boldsymbol{\sigma})) \\ &= -\underline{\kappa}||\boldsymbol{\sigma}|| \\ &= -\sqrt{2}\underline{\kappa}V^{\frac{1}{2}}. \end{aligned} \tag{15}$$

Based on the analysis process given above, if $\underline{\kappa} = min(\kappa_i) > 0$, then the system tracking error $\boldsymbol{e}_1$ will converge to the sliding mode surface $\boldsymbol{\sigma} = 0$ in finite time, which is

$$\begin{aligned} \boldsymbol{\sigma} &= \ddot{\boldsymbol{q}}_r - \boldsymbol{M}_0^{-1}(\boldsymbol{\eta}_1)\boldsymbol{u}(t) + \boldsymbol{F}(\boldsymbol{\eta}_1, \hat{\boldsymbol{\eta}}_2) \\ &\quad + \hat{\boldsymbol{\eta}}_3 + \boldsymbol{\lambda}_2\hat{\boldsymbol{\eta}}_2 + \boldsymbol{\lambda}_1\boldsymbol{\eta}_1 \\ &= \boldsymbol{0}. \end{aligned} \tag{16}$$

Reorganize the above formula, we can get:

$$\begin{aligned} &\ddot{\boldsymbol{q}}_r - \boldsymbol{M}_0^{-1}(\boldsymbol{\eta}_1)\boldsymbol{u}(t) + \boldsymbol{F}(\boldsymbol{\eta}_1, \hat{\boldsymbol{\eta}}_2) + \hat{\boldsymbol{\eta}}_3 + \boldsymbol{\lambda}_2\hat{\boldsymbol{\eta}}_2 + \boldsymbol{\lambda}_1\boldsymbol{\eta}_1 \\ &\quad = \ddot{\boldsymbol{q}}_r - \boldsymbol{M}_0^{-1}(\boldsymbol{\eta}_1)\boldsymbol{u}(t) + \boldsymbol{F}(\boldsymbol{\eta}_1, \boldsymbol{\eta}_2) + \boldsymbol{\eta}_3 + \boldsymbol{\lambda}_2\boldsymbol{\eta}_2 + \boldsymbol{\lambda}_1\boldsymbol{\eta}_1 \\ &\qquad + (\boldsymbol{F}(\boldsymbol{\eta}_1, \hat{\boldsymbol{\eta}}_2) - \boldsymbol{F}(\boldsymbol{\eta}_1, \boldsymbol{\eta}_2)) + (\hat{\boldsymbol{\eta}}_3 - \boldsymbol{\eta}_3) + \boldsymbol{\lambda}_2(\hat{\boldsymbol{\eta}}_2 - \boldsymbol{\eta}_2) \\ &\quad = \dot{\boldsymbol{\eta}}_2 + \boldsymbol{\lambda}_2\boldsymbol{\eta}_2 + \boldsymbol{\lambda}_1\boldsymbol{\eta}_1 \\ &\qquad + (\boldsymbol{F}(\boldsymbol{\eta}_1, \hat{\boldsymbol{\eta}}_2) - \boldsymbol{F}(\boldsymbol{\eta}_1, \boldsymbol{\eta}_2)) + (\hat{\boldsymbol{\eta}}_3 - \boldsymbol{\eta}_3) + \boldsymbol{\lambda}_2(\hat{\boldsymbol{\eta}}_2 - \boldsymbol{\eta}_2) \\ &\quad = \ddot{\boldsymbol{e}}_1 + \boldsymbol{\lambda}_2\dot{\boldsymbol{e}}_1 + \boldsymbol{\lambda}_1\boldsymbol{e}_1 \\ &\qquad + (\boldsymbol{F}(\boldsymbol{\eta}_1, \hat{\boldsymbol{\eta}}_2) - \boldsymbol{F}(\boldsymbol{\eta}_1, \boldsymbol{\eta}_2)) + (\hat{\boldsymbol{\eta}}_3 - \boldsymbol{\eta}_3) + \boldsymbol{\lambda}_2(\hat{\boldsymbol{\eta}}_2 - \boldsymbol{\eta}_2) \\ &\quad = \boldsymbol{0}. \end{aligned} \tag{17}$$

When the coefficient $\lambda_{ij} > 0$, the following system

$$\ddot{\boldsymbol{e}}_1 + \boldsymbol{\lambda}_2\dot{\boldsymbol{e}}_1 + \boldsymbol{\lambda}_1\boldsymbol{e}_2 = \boldsymbol{0}. \tag{18}$$

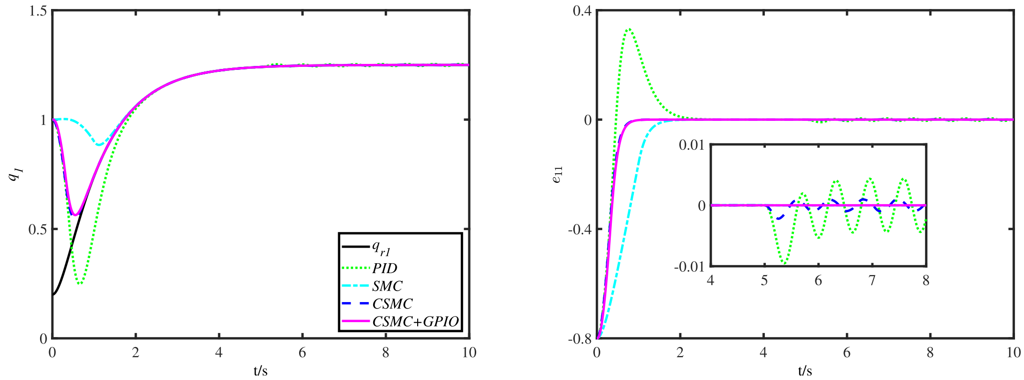

FIGURE 2. Curves of tracking trajectory q_1 and tracking error e_{11}.

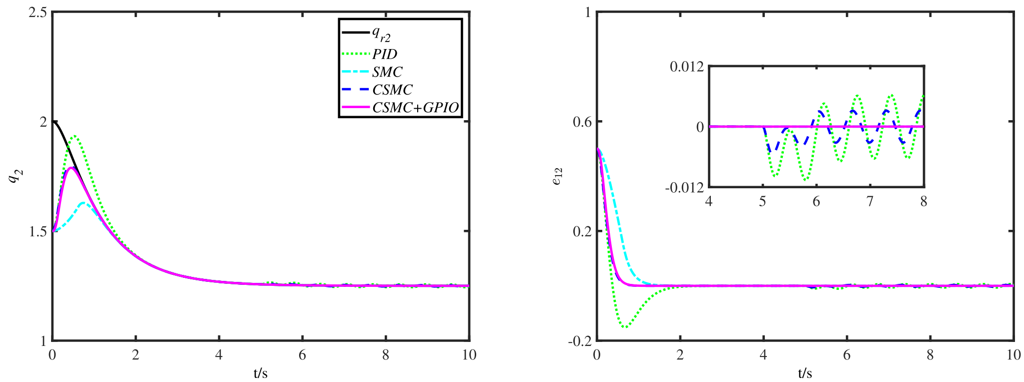

FIGURE 3. Curves of tracking trajectory q_2 and tracking error e_{12}.

is asymptotically stable. Combining formula (18) and the Lemma 5.5 in literature [41], it can be concluded that system (17) is ISS. Since estimate $\hat{\boldsymbol{\eta}}_i$ of observer (10) will asymptotically converge to its real value $\boldsymbol{\eta}_i$, which means $\lim_{t\to\infty}(\hat{\boldsymbol{\eta}}_i - \boldsymbol{\eta}_i) = \mathbf{0}$. Based on **Lemma 1**, it can be seen that system (17) satisfies the condition that the input becomes zero asymptotically, then we can get $\lim_{t\to\infty} \boldsymbol{e}_1(t) = \mathbf{0}$, which means system output $\boldsymbol{q}$ will asymptotically converge to $\boldsymbol{q}_r$. The proof is completed.

Remark 3: Compared with the traditional SMC method (6) and CSMC method (8), the recommended CSMC+GPIO method has the following advantages: 1) The proposed control algorithm has a continuous control behavior; 2) Due to the introduction of time-varying disturbance estimation $\hat{\boldsymbol{\eta}}_3$, control gain κ only needs to meet the conditions $min(\kappa_i) > 0$, which theoretically reduces the steady-state tracking error; 3) Based on the estimated values of unmeasurable states and disturbances, the new sliding mode surface (11) is constructed, which not only reduces the computational burden of the controller but also simplifies the theoretical analysis process compared with the approach in [23].

V. TEST RESULTS AND COMPARISON

A two-link rigid robot is shown in Fig. 1, and the mathematical model of the two-link rigid robot is given as follows [42]:

$$\begin{bmatrix}\alpha_{11}(q_2) & \alpha_{12}(q_2)\\ \alpha_{21}(q_2) & \alpha_{22}(q_2)\end{bmatrix}\begin{bmatrix}\ddot{q}_1\\ \ddot{q}_2\end{bmatrix} + \begin{bmatrix}-\beta_{12}(q_2)\dot{q}_1^2 - 2\beta_{12}(q_2)\dot{q}_1\dot{q}_2\\ \beta_{12}(q_2)\dot{q}_1^2\end{bmatrix} + \begin{bmatrix}\gamma_1(q_1,q_2)g\\ \gamma_1(q_1,q_2)g\end{bmatrix} = \begin{bmatrix}u_1\\ u_2\end{bmatrix} + \begin{bmatrix}d_1(t)\\ d_2(t)\end{bmatrix}, \tag{19}$$

where $\alpha_{11}(q_2) = (m_1+m_2)l_1^2 + m_2l_2^2 + 2m_2l_1l_2cos(q_2) + J_1$, $\alpha_{12}(q_2) = \alpha_{21}(q_2) = m_2l_2^2 + m_2l_1l_2cos(q_2)$, $\alpha_{22}(q_2) = m_2l_2^2 + J_2$, $\beta_{12}(q_2) = m_2l_1l_2sin(q_2)$, $\gamma_1(q_1,q_2) = (m_1+m_2)l_1cos(q_2)+m_2l_2cos(q_1+q_2)$, $\gamma_2(q_1,q_2) = m_2l_1l_2cos(q_1+q_2)$. The model parameters in the above formula are: $m_1 = 0.5Kg$, $m_2 = 1.5Kg$, $l_1 = 1m$, $l_2 = 0.8m$, $J_1 = 5Kg\cdot m$, $J_2 = 5Kg\cdot m$, $g = 9.8N\times s$.

The reference trajectory is set as: $q_{r1} = 1.25-(7/5)e^{-t} + (7/20)e^{-4t}$, $q_{r2} = 1.25+e^{-t}-(1/4)e^{-4t}$. The external disturbance is set as:$[d_1, d_2]^T = [5, 5]^T + [5sin(10t), 5cos(10t)]^T$. The initial state of the system is set as: $q_1(0) = 1.0$, $q_2(0) = 1.5$, $\dot{q}_1(0) = 0$, $\ddot{q}_2(0) = 0$, The limit value of the control signal is satisfying ± 50.

In order to verify and illustrate the advantages of the recommended control methods, the PID, SMC, and CSMC

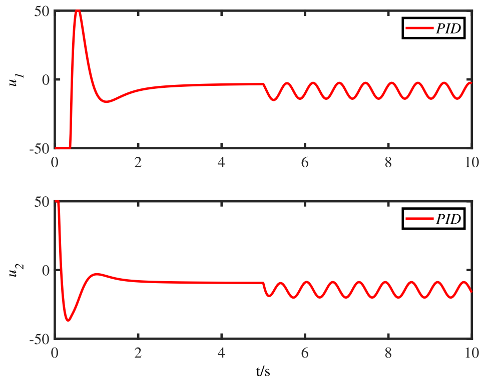

(a) Control curves under the PID control scheme

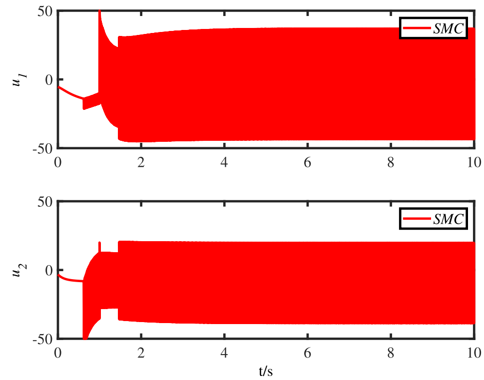

(b) Control curves under the SMC control scheme

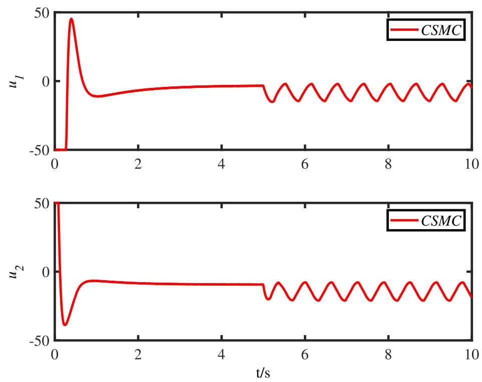

(c) Control curves under the CSMC control scheme

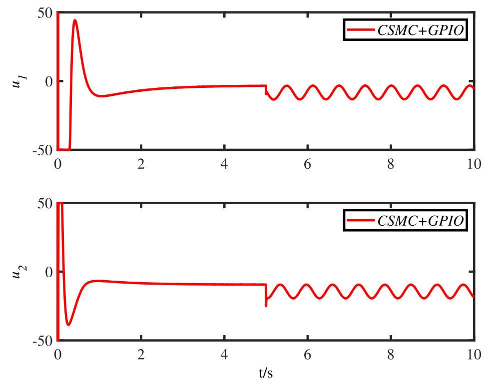

(d) Control curves under the CSMC+GPIO control scheme

FIGURE 4. Control curves under different control schemes.

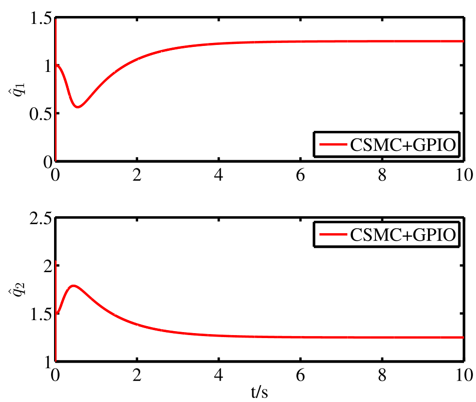

(a) Estimated curves of q_1 and q_2

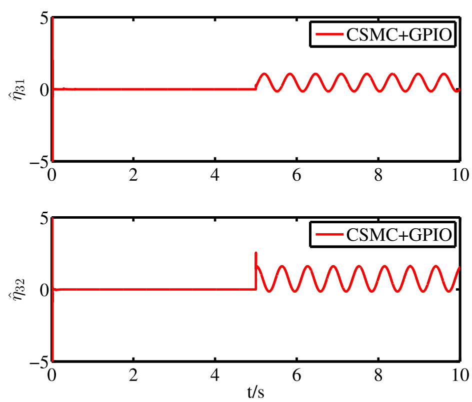

(b) Estimated curves of η_{31} and η_{32}

FIGURE 5. Estimated curves under the CSMC+GPIO control scheme.

schemes are set as contrast control methods in the test. The PID control method is designed as:

$$\boldsymbol{u}(t) = \boldsymbol{M}_0(\boldsymbol{e})(\ddot{\boldsymbol{q}}_r + \boldsymbol{F}(\boldsymbol{e}, \dot{\boldsymbol{e}}) + \boldsymbol{k}_d\dot{\boldsymbol{e}} + \boldsymbol{k}_p\boldsymbol{e} + \boldsymbol{k}_i\int_0^t e d\sigma), \tag{20}$$

where $\boldsymbol{k}_D = diag(k_{D1}, K_{D2})$, $\boldsymbol{k}_P = diag(k_{P1}, k_{P2})$, $\boldsymbol{k}_I = diag(k_{I1}, K_{I2})$, $\boldsymbol{e} = \boldsymbol{q}_r - \boldsymbol{q}$.

To make a fair comparison, first of all, let the control input of the four control algorithms has the same saturation limit. Secondly, by adjusting the parameters of each control algorithm, let all the closed-loop systems obtain relatively good performance. The control parameters of the four controllers are shown in Tab. 1. Fig. 2-Fig. 4 show the comparison test results of different control methods on the two-link rigid robot system. The trajectory tracking curve q_1 and tracking error curve $e_{11} = q_{r1} - q_1$ of the first joint under different control methods are shown in Fig. 2. The trajectory tracking curve q_2 and tracking error curve $e_{12} = q_{r2} - q_2$ of the second joint under different control methods are shown in Fig. 3. The control input curves u_1 and u_2 of the robot under different control strategies are shown in Fig. 4. Fig. 5 lists the estimated curves $\hat{q}_1$, $\hat{q}_2$, $\hat{\eta}_{31}$, and $\hat{\eta}_{32}$ of the system under the CSMC+GPIO control scheme.

As can be seen from the tracking curves in Fig. 2 and Fig. 3, four control methods can complete the trajectory tracking task well, however, when the robot runs under the driven of the PID control method, the tracking trajectory has a large overshoot in the initial stage, and the tracking trajectory under CSMC and CSMC+GPIO methods can quickly track the reference trajectory.

Meanwhile, when the system runs at 5 s, an external disturbance $[d_1, d_2]^T$ is applied. It is obvious that there is a large position fluctuation in the system under the PID control method. The above pictures also indicate that the anti-disturbance ability of the robot is the worst when the PID control method is used, it is stronger when the CSMC is used, and it is the strongest when the traditional SMC and CSMC+GPIO are used. However, it can be deduced from Fig. 4(b) that the curves of control input have relatively large chattering when the robot uses the traditional SMC methods, which may cause permanent damage to the system actuator. Therefore, the recommended CSMC+GPIO method not only has a continuous control law but also enables the system to obtain fast tracking performance and strong anti-disturbance performance.

VI. CONCLUSION

The trajectory tracking of disturbed robots has been studied in this paper. First, two trajectory tracking controllers based on the traditional SMC and CSMC methods have been designed respectively by utilizing the robot dynamic model, and the problems existing in these two control methods have been analyzed at the same time. In order to solve these problems, the trajectory tracking control scheme combining the GPIO and CSMC has been proposed, and the stability of the closed-loop system has also been guaranteed by a Lyapunov function. Finally, four control methods, covering the PID control, traditional SMC, CSMC, and CSMC+GPIO approaches, have been tested respectively on the two-degree-of-freedom robot. The results verify that the recommended control method has faster tracking performance and stronger anti-disturbance ability. In the future, we would like to further validate the present control scheme on some actual robotic arm platforms.

REFERENCES

[1] H. Wang, Y. Pan, S. Li, and H. Yu, "Robust sliding mode control for robots driven by compliant actuators," *IEEE Trans. Control Syst. Technol.*, vol. 27, no. 3, pp. 1259–1266, May 2019.

[2] H. Yu, S. Huang, G. Chen, Y. Pan, and Z. Guo, "Human–robot interaction control of rehabilitation robots with series elastic actuators," *IEEE Trans. Robot.*, vol. 31, no. 5, pp. 1089–1100, Oct. 2015.

[3] R. Ham, T. Sugar, B. Vanderborght, K. Hollander, and D. Lefeber, "Compliant actuator designs," *IEEE Robot. Autom. Mag.*, vol. 16, no. 3, pp. 81–94, Sep. 2009.

[4] H. Yu, S. Huang, G. Chen, and N. Thakor, "Control design of a novel compliant actuator for rehabilitation robots," *Mechatronics*, vol. 23, no. 8, pp. 1072–1083, Dec. 2013.

[5] X. P. Shi and S. R. Liu, "A survey of trajectory tracking control for robot manipulators," *Control Eng. China*, vol. 18, no. 1, pp. 116–122, Jun. 2011.

[6] J. F. Engelberger, *Robotics in Practice: Management and Applications of Industrial Robots*. London, U.K.: Springer, 2012.

[7] T. Shu, S. Gharaaty, W. Xie, A. Joubair, and I. A. Bonev, "Dynamic path tracking of industrial robots with high accuracy using photogrammetry sensor," *IEEE/ASME Trans. Mechatronics*, vol. 23, no. 3, pp. 1159–1170, Jun. 2018.

[8] E. Pereira, S. S. Aphale, V. Feliu, and S. O. R. Moheimani, "Integral resonant control for vibration damping and precise tip-positioning of a single-link flexible manipulator," *IEEE/ASME Trans. Mechatronics*, vol. 16, no. 2, pp. 232–240, Apr. 2011.

[9] X. Li, Y. Pan, G. Chen, and H. Yu, "Continuous tracking control for a compliant actuator with two-stage stiffness," *IEEE Trans. Autom. Sci. Eng.*, vol. 15, no. 1, pp. 57–66, Jan. 2018.

[10] Y. Pan, X. Li, H. Wang, and H. Yu, "Continuous sliding mode control of compliant robot arms: A singularly perturbed approach," *Mechatronics*, vol. 52, pp. 127–134, Jun. 2018.

[11] J. N. Yun and J.-B. Su, "Design of a disturbance observer for a two-link manipulator with flexible joints," *IEEE Trans. Control Syst. Technol.*, vol. 22, no. 2, pp. 809–815, Mar. 2014.

[12] M. W. Spong, S. Hutchinson, and M. Vidyasagar, *Robot Modeling and Control*, vol. 3. New York, NY, USA: Wiley, 2006.

[13] J. Su, J. Yang, and S. Li, "Continuous finite-time anti-disturbance control for a class of uncertain nonlinear systems," *Trans. Inst. Meas. Control*, vol. 36, no. 3, pp. 300–311, May 2014.

[14] J. Zhai and G. Xu, "A novel non-singular terminal sliding mode trajectory tracking control for robotic manipulators," *IEEE Trans. Circuits Syst. II, Exp. Briefs*, vol. 68, no. 1, pp. 391–395, Jan. 2021.

[15] Q. Hou and S. Ding, "Finite-time extended state observer based super-twisting sliding mode controller for PMSM drives with inertia identification," *IEEE Trans. Transport. Electrific.*, early access, Oct. 27, 2021, doi: 10.1109/TTE.2021.3123646.

[16] Q. Hou, S. Ding, X. Yu, and K. Mei, "A super-twisting-like fractional controller for SPMSM drive system," *IEEE Trans. Ind. Electron.*, vol. 69, no. 9, pp. 9376–9384, Sep. 2022.

[17] J. Yang, T. Li, C. Liu, S. Li, and W.-H. Chen, "Nonlinearity estimator-based control of a class of uncertain nonlinear systems," *IEEE Trans. Autom. Control*, vol. 65, no. 5, pp. 2230–2236, May 2020.

[18] L. Liu, S. Ding, and X. Yu, "Second-order sliding mode control design subject to an asymmetric output constraint," *IEEE Trans. Circuits Syst. II, Exp. Briefs*, vol. 68, no. 4, pp. 1278–1282, Apr. 2021.

[19] K. Mei and S. Ding, "HOSM controller design with asymmetric output constraints," *Sci. China Inf. Sci.*, vol. 65, no. 8, pp. 1–2, Aug. 2022.

[20] J. Yuan, S. Ding, and K. Mei, "Fixed-time SOSM controller design with output constraint," *Nonlinear Dyn.*, vol. 102, no. 3, pp. 1567–1583, 2020.

[21] M. A. Khosravi and H. D. Taghirad, "Dynamic modeling and control of parallel robots with elastic cables: Singular perturbation approach," *IEEE Trans. Robot.*, vol. 30, no. 3, pp. 694–704, Jun. 2014.

[22] Z. Zhao, J. Yang, S. Li, X. Yu, and Z. Wang, "Continuous output feedback TSM control for uncertain systems with a DC–AC inverter example," *IEEE Trans. Circuits Syst. II, Exp. Briefs*, vol. 65, no. 1, pp. 71–75, Jan. 2017.

[23] Y. Feng, F. Han, and X. Yu, "Chattering free full-order sliding-mode control," *Automatica*, vol. 50, no. 4, pp. 1310–1314, 2014.

[24] R. J. Liu, M. Wu, G. P. Liu, J. She, and C. Thomas, "Active disturbance rejection control based on an improved equivalent-input-disturbance approach," *IEEE/ASME Trans. Mechatronics*, vol. 18, no. 4, pp. 1410–1413, Aug. 2013.

[25] T. Jiang, C. Huang, and L. Guo, "Control of uncertain nonlinear systems based on observers and estimators," *Automatica*, vol. 59, pp. 35–47, Sep. 2015.

[26] J. Sun, J. Yang, W. X. Zheng, and S. Li, "GPIO-based robust control of nonlinear uncertain systems under time-varying disturbance with application to DC–DC converter," *IEEE Trans. Circuits Syst. II, Exp. Briefs*, vol. 63, no. 11, pp. 1074–1078, Nov. 2016.

[27] X. Li, Y. Pan, G. Chen, and H. Yu, "Adaptive human–robot interaction control for robots driven by series elastic actuators," *IEEE Trans. Robot.*, vol. 33, no. 1, pp. 169–182, Feb. 2017.

[28] Y. Cao and X. Chen, "Disturbance-observer-based sliding-mode control for a 3-DOF nanopositioning stage," *IEEE/ASME Trans. Mechatronics*, vol. 19, no. 3, pp. 924–931, Jun. 2014.

[29] J. Yang, S. Li, and X. Yu, "Sliding-mode control for systems with mismatched uncertainties via a disturbance observer," *IEEE Trans. Ind. Electron.*, vol. 60, no. 1, pp. 160–169, Jan. 2013.

[30] S. E. Talole, J. P. Kolhe, and S. B. Phadke, "Extended-state-observer-based control of flexible-joint system with experimental validation," *IEEE Trans. Ind. Electron.*, vol. 57, no. 4, pp. 1411–1419, Apr. 2010.

[31] W. Chen, J. Yang, L. Guo, and S. Li, "Disturbance-observer-based control and related methods-an overview," *IEEE Trans. Ind. Electron.*, vol. 63, no. 2, pp. 1083–1095, Feb. 2016.

[32] H. Wang, W. Peng, X. Tan, J. Sun, X. Tang, and I.-M. Chen, "Robust output feedback tracking control for flexible-joint robots based on CTSMC technique," *IEEE Trans. Circuits Syst. II, Exp. Briefs*, vol. 68, no. 6, pp. 1982–1986, Jun. 2021.

[33] J. Sun, J. Yang, and S. Li, "Reduced-order GPIO based dynamic event-triggered tracking control of a networked one-DOF link manipulator without velocity measurement," *IEEE/CAA J. Autom. Sinica*, vol. 7, no. 3, pp. 725–734, May 2020.

[34] X.-H. Chang and G.-H. Yang, "Nonfragile H_∞ filter design for T–S fuzzy systems in standard form," *IEEE Trans. Ind. Electron.*, vol. 61, no. 7, pp. 3448–3458, Jul. 2014.

[35] X.-H. Chang and Y. Liu, "Robust H_∞ filtering for vehicle sideslip angle with quantization and data dropouts," *IEEE Trans. Veh. Technol.*, vol. 69, no. 10, pp. 10435–10445, Oct. 2020.

[36] H. Wang, S. Li, J. Yang, and X. Zhou, "Continuous sliding mode control for permanent magnet synchronous motor speed regulation systems under time-varying disturbances," *J. Power Electron.*, vol. 16, no. 4, pp. 1324–1335, 2016.

[37] S. Li, K. Zong, and H. Liu, "A composite speed controller based on a second-order model of permanent magnet synchronous motor system," *Trans. Inst. Meas. Control*, vol. 33, no. 5, pp. 522–541, 2011.

[38] Y. Shtessel, C. Edwards, L. Fridman, and A. Levant, *Sliding Mode Control and Observation*, vol. 10. New York, NY, USA: Springer, 2014.

[39] H. Wang, S. Li, Q. Lan, Z. Zhao, and X. Zhou, "Continuous terminal sliding mode control with extended state observer for PMSM speed regulation system," *Trans. Inst. Meas. Control*, vol. 39, no. 8, pp. 1195–1204, Aug. 2017.

[40] Q. Hou and S. Ding, "GPIO based super-twisting sliding mode control for PMSM," *IEEE Trans. Circuits Syst. II, Exp. Briefs*, vol. 68, no. 2, pp. 747–751, Feb. 2021.

[41] H. K. Khalil, *Nonlinear Systems*, vol. 115, 3rd ed. Upper Saddle River, NJ, USA: Prentice-Hall, 2002.

[42] Y. Feng, X. Yu, and Z. Man, "Non-singular terminal sliding mode control of rigid manipulators," *Automatica*, vol. 38, no. 12, pp. 2159–2167, 2002.